International Journal of GEOMATE, Aug., 2024 Vol.27, Issue 120, pp.17-26
ISSN: 2186-2982 (P), 2186-2990 (O), Japan, DOI: https://doi.org/10.21660/2024.120.4382
Geotechnique, Construction Materials and Environment

EFFECTS OF THE CONSTRUCTION OF DEEP FOUNDATION PITS BY THE OPEN EXCAVATION METHOD ON THE DEFORMATION OF NEIGHBORING HOUSES

*Nguyen Hong Nam[1]

[1]Division of Geotechnical Engineering, Thuyloi University, Vietnam

*Corresponding Author, Received: 17 Jan. 2024, Revised: 29 May 2024, Accepted: 13 June 2024

ABSTRACT: The open excavation method is a common technique for constructing shallow underground works in foundation pits. The incident of settlement and cracking of resident houses around a 2-basement deep foundation pit of a 26-storey twin tower office building constructed in Hanoi by the open excavation method has been studied. The methods employed were a combination of site investigation and numerical and analytical simulations of a real problem. For the numerical simulation problem, two sections, North-South and East-West, were analyzed using the finite element method, plane strain problem, according to different excavation stages. The simulation results showed that the measures to protect the western slope of the foundation pit by using only bored piles without reinforcing the slope of resident houses adjacent to the excavation pit led to large ground deformation, endangering the stability of the pit and the structure of the adjacent houses. The above-simulated ground settlement results were consistent with those calculated by the method of the beam on an elastic foundation.

Keywords: Open excavation method, Settlement, Deep foundation pit, Finite element, Bored piles.

1. INTRODUCTION

The open excavation method is a common technique for constructing shallow underground works in foundation pits. This involves digging a pit from the ground, which is then backfilled with soil. The open excavation method offers advantages such as the flexibility to use various construction machines, ease of waterproofing for underground works, and simplicity and effectiveness in construction near the outer wall of existing underground structures. This method is particularly advantageous for large, shallow underground structures on the ground. However, it has limitations in urban areas, including: a) Occupying significant land space, causing noise, and leading to traffic congestion. b) There is a need to stabilize the pit walls and bottom. c) Potential impact on the foundation of existing structures, resulting in reduced resistance or deformation. d) Issues related to immigration and land clearance. e) Soil displacement and subsidence of existing structures [1]. Lately, there has been a growing utilization of servo steel struts in the construction of deep foundation pits where precise management of the surrounding deformation caused by excavation is essential [2,3].

In cities like Hanoi and Ho Chi Minh, the construction of deep excavations alongside pre-existing buildings is a common practice. One critical concern during such excavation is the potential deformation of neighboring structures. Failure to address this issue effectively, especially in large-scale projects, may lead to unforeseen disasters for residents around the construction sites.

Various methods have been employed to predict ground displacement adjacent to excavations, including the observation method [4], beam on the elastic foundation [5], empirical methods [6-8], semi-empirical methods [9-11], and the finite element method [12].

The analytical (closed-form) method for estimating ground movements is quick and easy to apply for predicting excavation-induced ground deformations. However, it is generally limited to simple conditions, such as half-space homogeneous linear elastic grounds. The empirical method is also convenient for predicting surface ground deformation but depends on specific soil conditions. Although the finite element method is a powerful tool that can use advanced soil models to calculate ground and structure deformations under very complex boundary and loading conditions, it requires extensive calibration of many model parameters using advanced soil testing and complex stress loading paths. However, fully calibrating all advanced soil model parameters is time-consuming and constrained by the limitations of the testing apparatus and measuring devices.

The analysis of deformation in existing building foundations adjacent to a deep excavation site during foundation pit construction should be an integral part of the foundation design process. Factors influencing ground settlement, such as excavation depth, distance from the building, soil properties, and building height, must be taken into account. Through this analysis, key influencing parameters and effective mitigation measures can be identified to enhance building safety and minimize damage.

2. RESEARCH SIGNIFICANCE

The present study focuses on the effect of constructing the foundation pit on the deformation of adjacent structures. This article aims to calculate ground displacements adjacent to the excavation of the Golden Westlake project based on geotechnical investigation data [13] and stage construction measures. Finite element and analytical analyses were conducted to evaluate and compare the extent of ground displacements that could impact nearby residential buildings due to the excavation work. Based on the calculation results, the project investor and related parties have a basis to determine the compensation level for the residents around the project area affected by the settlement caused by the foundation excavation process.

3. MATERIALS AND METHODS

3.1. Golden Westlake Project

The Golden Westlake twin tower office building project in Hanoi is located at 151 Thuy Khue Street, Tay Ho district, Hanoi city. The project consists of 26 above-ground floors and 2 basement levels, with a total construction area of approximately 70,180 square meters.

At the time of this study, the project was under construction. The deep foundation pit, measuring 54.4 m wide, 102 m long, and 9.735 m deep, was completed using the open excavation method [14]. The reinforcing excavation slopes were implemented during different construction periods. It is important to note that the excavation work was performed after the installation of drilled pile foundations (Fig. 1b).

3.1.1. Excavation slope protection at the East and West sides

The excavation slopes were protected using a combination of bored pile foundations (D800mm, C25 concrete, and 14D25 steel) and ground anchors. The top of the pile foundations is at -4.0 meters, and the pile tips extend to -15.70 meters. The spacing between two rows of pile foundations in the East-West direction is 2.4 meters.

The area of the excavation slope, from elevation -4.0 meters to the natural ground level (+0.0m), is reinforced with a 10cm thick layer of C20 concrete and steel mesh (ϕ6.5, @200x200mm). A 1000x500mm C25 concrete beam connects the tops of the front row of D800 bored pile foundations at a depth of -4.0 meters. The tops of the two rows of pile foundations are interconnected by a reinforced concrete beam. The protective beams for the nearby residential structures at the natural ground level come in various sizes (600x300mm, 500x300mm) and are constructed with C20 concrete and steel reinforcement (6ϕ20, ϕ6.5, @200).

Three anchor rows (ground nails) have lengths ranging from 5-6m, a diameter of 100mm, and are inclined at 10 degrees to the horizontal axis. The steel anchors have a diameter of D20. The holes for the anchors are filled with grout (P.O 32.5 cement, water-cement ratio of 0.5). The distance between anchor rows vertically is 1.5m, and horizontally is 1.5m.

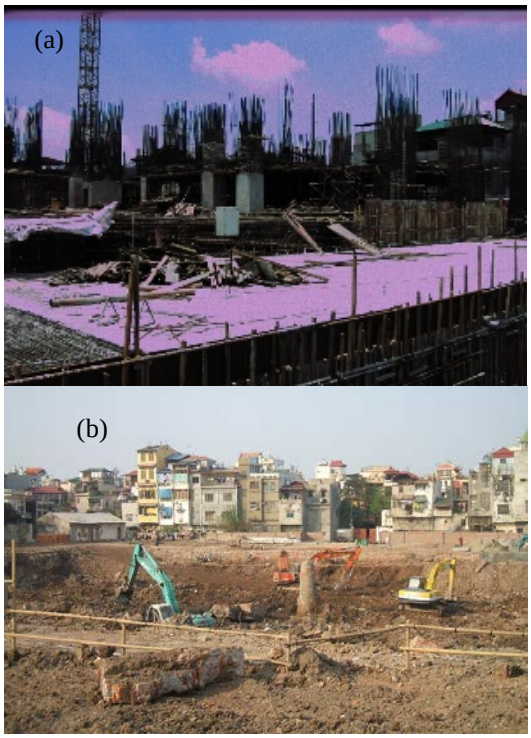

Fig. 1 Excavation during construction

3.1.2. Excavation slope protection at the South and North sides

For both sides of the excavation slopes, facing north and south, the contractor implements the slope protection using a ground anchoring system. As per the design, the ground is excavated into layers to form the slope at a 63.5-degree angle, reinforced by six rows of retaining steel anchors. The surface of the slope is poured with 10cm thick C20 concrete containing D6.5 steel mesh with a grid size of 200x200mm. The anchoring system uses D20 steel, 9-12m long, encased in sprayed concrete, with anchor diameters ranging from 10-13cm. The distance between rows of steel anchors is 1.5m, and the distance between anchors within a row is 1.2m. Three rows of drainage pipes are horizontally embedded deep in the ground to drain seepage, spaced 3m apart horizontally and vertically, creating drainage channels at the base of the slope to collect water.

3.1.3. Bored pile foundation

For the foundation, bored piles are used with C40 grade concrete, and the reinforcing steel has a yield strength of Ra=235 MPa (for D<10) and Ra=390 MPa (for D>10). There are two types of bored piles with different diameters: D=1200mm and 1000mm. The pile cap elevation is -9.735m, and the pile tip elevations are -50.45m (D1200mm) and -39.85m (D1000mm).

3.1.4. Construction sequence

The excavation work for the pit was carried out after completing the bored pile construction for the project's foundation.

Initially, two rows of bored piles were constructed for retaining, with a diameter of 800mm and a length of 11.7m, and the pile heads were positioned at a depth of 4.0m below the ground level.

The pit excavation in the central area was done in phases: Phase 1 dug to -4.0m, Phase 2 to -8.0m, and Phase 3 to the full depth of -9.735m. During the excavation in the central pit area, the border surfaces were dug and reinforced in layers from top to bottom.

Excavation and construction of the supporting pile system, the ground anchors on the Eastern and Western sides adjacent to the red boundary:

-Excavation and creating a sloped surface to a depth of -4.0m, reinforced by ground anchors in the pit wall in layers. In the area adjacent to the fence where ground anchors were not used, a beam system was constructed in place of the slope. Drainage pipes were placed underground to create water drainage channels at the base of the slope.

-Constructing a beam system to support the head of the piles, providing a smooth surface for construction activities.

-Excavating a vertical slope with the pit's depth reaching bottom of the foundation pit (-9.735m).

-Pouring concrete with steel mesh between the support piles, creating drainage channels at the base of the pit.

Excavation and construction of the sloped surface, reinforced by ground anchors on the Northern and Southern sides in layers:

-Digging and forming a sloped surface 1.8m deep, drilling and creating rows of ground anchors 1.5m from the ground, constructing a concrete surface with 1cm thick steel mesh. Drainage pipes were placed horizontally at a depth of 4m, 3m apart, for seepage drainage.

-Constructing similar sloped layers at depths of 3.3m, 4.8m, 6.3m, 7.8m, and 9.3m. The ground anchor rows were positioned 3m, 4.5m, 6m, 7.5m, and 9m from the ground, anchored 12m deep. Three rows of underground drainage pipes placed 3m apart in depth were installed for seepage drainage.

-Excavating to a depth of -9.735m, placing steel mesh and pouring a 100mm thick concrete layer, creating drainage channels at the base of the pit.

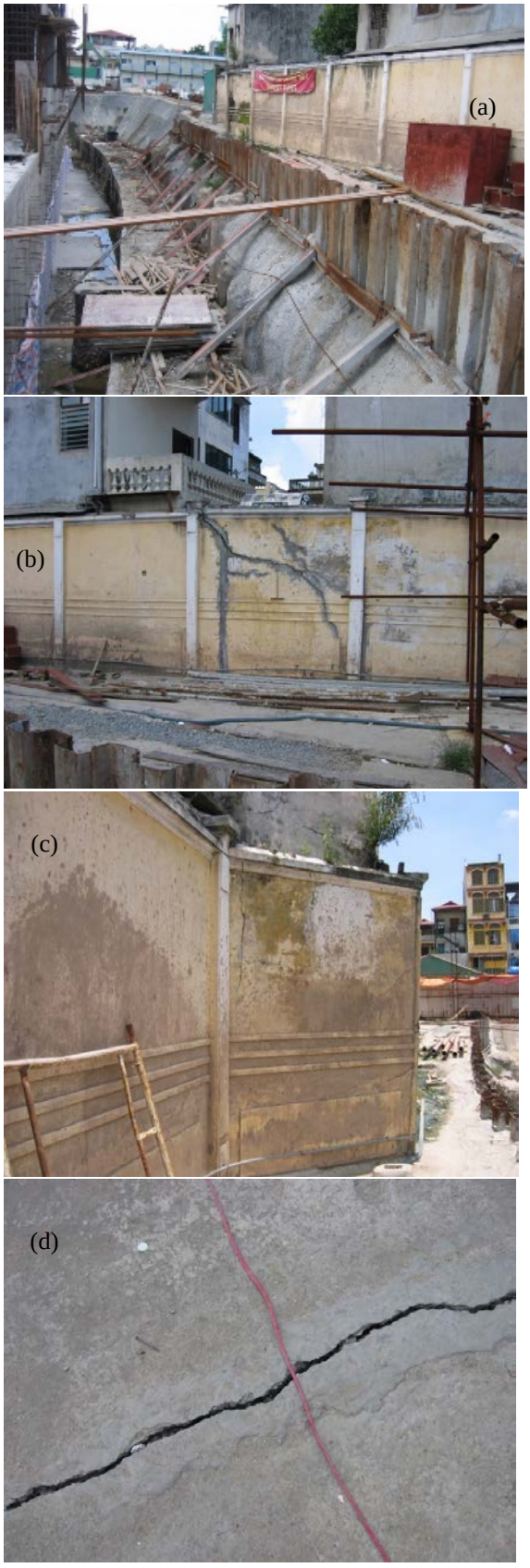

Fig. 2 Excavation slope on the West side

Table 1 Foundation soil description

Layer	Description
1	Made ground, soft-firm sandy lean clay (CL) with pieces of bricks and organic materials
2	Very soft brownish-blackish grey lean clay with sands and organic materials
3	Firm brownish grey lean clay (CL)
4	Soft yellowish-brownish grey lean clay with sands and organic materials (CL)
5	Firm strong brownish grey sandy clay, alternative some lens, thin layers of sand and organic materials (CL)
6	Stiff brownish grey lean clay with sands, alternative some lens and thin layers of sand (CL)
7	Stiff greenish-yellowish grey, brown sandy lean clay (CL)
8	Medium dense ash-light greenish grey silty sand (SM)
9	Medium dense poorly graded sand with silts and gravels with coarse sands
10	Very dense well graded light greenish-whitish and yellowish grey sand with silts and gravels-very dense poorly graded light greenish-yellowish grey gravel (SW-SM and GP).
11	Plasticity brownish grey clayey sand (SC), with small gravels and sands at some places
12	Very dense well-graded light greenish-whitish and yellowish grey sand with silts and gravels-very dense poorly graded light greenish-yellowish grey gravel (SW-SM and GP)

Table 2 Soil properties of foundation

Soil layer /Properties	Layer 1	Layer 3	Layer 5	Layer 7
w (%)	33.3	31.6	32.7	28.0
γ (kN/m^3)	17.5	17.8	17.8	19.3
GS	2.65	2.66	2.66	2.67
e	1.023	0.97	0.985	0.768
S (%)	86.3	86.6	88.3	97.3
LL (%)	37.9	35.4	36.9	37.2
PL (%)	21.9	20.8	22.3	22.1
PI (%)	16	14.6	14.6	15.1
LI	0.71	0.74	0.71	0.39
φ (deg.)	9.50	6.50	9.00	16.00
c (kN/m^2)	11.00	8.00	12.00	19.00
a12(cm^2/kg)	0.065	0.058	0.055	0.030
k (m/day)	$5.62x10^{-4}$	$5.62x10^{-4}$	$5.62x10^{-4}$	$5.62x10^{-4}$
v	0.350	0.350	0.350	0.350
E (kN/m^2)	2489.85	2717.00	2887.00	4286.00

3.2. Site inspection

The site visit was conducted in June 2007 to observe the excavation. During the investigation, the foundation pit was completed, and superstructures were under construction (Fig. 1a). On-site, some sliding occurred on the western side of the excavation slope (Fig. 2a).

The impact of the foundation pit construction on nearby residential houses was observed, including ground cracks (Fig. 2d), boundary wall cracks (Fig. 2b), tilting toward the excavation (Fig. 2c), and settlement of the resident houses [14]. The construction of the foundation pit took place from November 2006 to April 2007 [14]. The contractor later used Larsen steel sheet piling to reinforce the West side of the excavation wall to limit ground surface deformation (Figure 2a).

Fig. 3 Excavation slopes at the a) East side and b) North side

The excavation slopes at the East side (Fig. 3a) and North side (Fig. 3b) were stable at the time of site visit. Some bamboo piles were reinforced at the bottom of excavation slope at the North side.

3.3. FEM modeling

3.3.1. Mesh

The deformation of the foundation pit is simulated using the finite element method, employing a 2D plane strain model. The Plaxis software, version 8 was employed [15]. Two cross-sections in the East-West and North-South directions were analyzed in full section since the plane strain problem is not symmetrical in geometry, geotechnical, surface loading and adjacent structures (Fig. 4). The analysis of both cross-sections was implemented by stage of excavation construction. Figure 4a and 4b shows two finite element meshes with 1,945 and 1602 triangular elements for the East-West and North-South cross-sections, respectively.

3.3.2. Soil data

Based on the geotechnical investigation record

[13], the foundation stratigraphy consists of 12 layers from the surface downward (Table 1).

The geotechnical properties of soil layers 1, 3, 5, and 7 are provided in Table 2. Deeper soil layers fall under the category of sandy soil (8, 9) or gravelly soil (10, 11, 12). Due to the absence of specific test data, tentative values are used based on the published sources [10, 15]: cohesion (c) = 1kPa, friction angle (ϕ) = 30 degrees, Poisson's ratio (v) = 0.3, and Young's modulus (E) = 10^4 kN/m². The soil is simulated using the Mohr-Coulomb model [15] for simplicity. Initial soil stresses were first calculated. The simulated layers included layers 1, 3, 5, and 7 through 12 from the top surface to the bottom (Fig. 4).

3.3.3. Ground water

A horizontal water drainage system with a length of 4000mm and a horizontal spacing of 3000mm, combined with drainage ditches, is used during construction. Therefore, it can be assumed that the groundwater level is lowered to an elevation of -10m from the natural ground level.

3.3.4. Structures

Bored piles, pile caps, and beams are modeled using plate elements. Anchors are modeled using anchor elements, and the anchor head is modeled using geogrid elements. Please note that according to the design, for the excavation towards the West, the area close to the residential buildings does not use anchors (Fig. 4a).

3.3.5. Surface loading

Distributed loads on the ground surface towards the East and West are assumed equally q=36kN/m^2 as equivalent to the three-story house load (Fig. 4a). Distributed loads on the ground surface towards the North are taken q=15.5 and 36kN/m^2 (Fig. 4b). No consideration applied for distributed load on the ground surface towards the South.

3.3.6. Construction phase

The excavation process takes place after completing the construction of the bored pile foundation system. The excavation process encompasses various stages such as digging the central area, constructing the eastern and western edges of the excavation, as well as the northern and southern edges.

The construction process for the eastern and western edges of the excavation includes the following elements: installation of two rows of bored pile foundations using reinforced concrete piles (D800mm, concrete grade C25, steel reinforcement 14D25) and reinforcing the slope using an anchoring system and covering the slope surface with reinforced concrete.

To simplify the calculations, the excavation process is divided into three primary stages as follows:

Stage 1: Excavation down to the elevation of -4.0m.
Stage 2: Excavation down to the elevation of -8.0m.
Stage 3: Excavation down to the elevation of -9.735m.

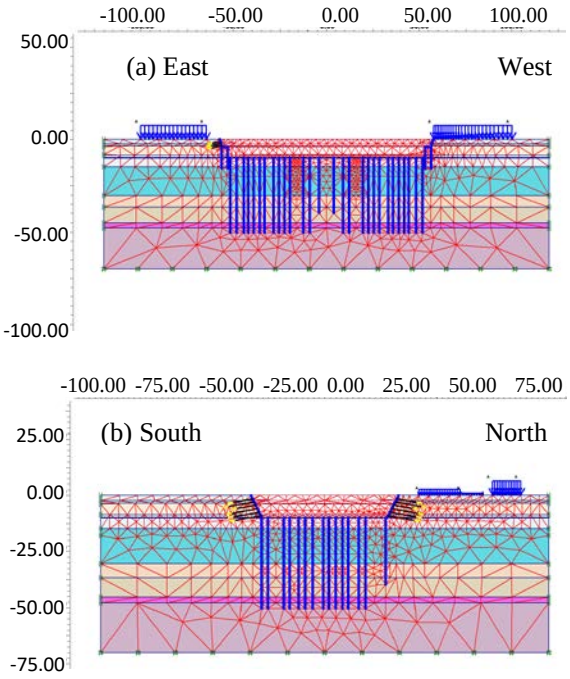

Fig. 4 Two analyzed cross-sections of East-West (a) and North-South (b)

Construction of the northern and southern edges of the excavation involves excavation and reinforcing the slope using an anchoring system and a layer of reinforced concrete.

To simplify the calculations, the construction process for the northern and southern edges can be divided into two main stages:

Stage 1: Excavation down to the elevation of -4.0m.
Stage 2: Excavation down to the elevation of -9.735m.

3.4. Beam on elastic foundation

The model of a building situated near a deep excavation is adopted in the form of a beam with a bending stiffness EJ (Fig. 5). The interaction between the building and underlying soil is represented by the working diagram of a beam on an elastic bed, the properties of which are described by a Winkler model as shown in Eqs. (1)-(3) [5].

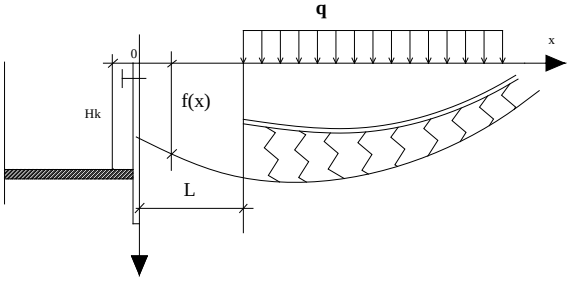

Fig. 5 Computational diagram for beam on elastic bed near deep excavation (not to the same scale)

$$S(x) = k_r \left[\delta \emptyset(x) + \frac{q}{k}\right] \quad (1)$$

$$\delta = \frac{A_1 f_1 H_k^5}{\left(\alpha^4 + A_1 H_k^4\right)} \quad (2)$$

$$A_1 = \frac{k}{EJ} \quad (3)$$

Where: S: Settlement; k: Coefficient of subsoil reaction (kN/m³);

EJ: Stiffness of the building, dependent on the number of floors (kNm²/m). The EJ values for slab, one story, three stories, five stories, 10 stories are 6.47×10^3, 2.00×10^7, 6.00×10^8, 6.98×10^8, 4.39×10^9 kN.m²/m, respectively.

q: Pressure at the foundation base at the bottom of the building's continuous foundation;

k_r: Coefficient considering the influence of the type of soil-retaining structure of the excavation, derived from observed actual building displacements near the excavation;

H_k: Depth of the excavation (m);

x: Coordinate of a point along the length of the building (m), where x=0 at the end of the building closest to the excavation.

4. RESULTS AND DISCUSSION

4.1. FEM simulation of East -West cross section

4.1.1. During the excavation phase down to the elevation of -4.0m

It can be observed from the calculation results that the maximum total displacement reaches approximately 22.0 cm. The maximum horizontal displacement reaches about 9.5 cm (Fig.6a). This value appears at the edge of the excavation towards the West, close to the elevation of -4.0m. The maximum vertical displacement reaches around 22.0 cm (Fig.6b). This value appears at the bottom of the excavation at the elevation of -4.0m when the soil experiences heaving. The maximum settlement at the natural ground level at the elevation of +0.0 is approximately 21.0 cm.

4.1.2. During the excavation phase down to the elevation of -8.0m

Figure 7 illustrates the deformation results of the excavation at the elevation of -8.0m. The total deformation of the structure reaches a maximum value of approximately 40.0 cm. The highest horizontal displacement measures around 23.3 cm at the western edge of the excavation (Fig. 7a). This value appears near the base of the excavation at the -8.0m level. The maximum vertical displacement reaches about 40.0 cm (Fig. 7b). This value appears at the base of the foundation, within a range of approximately 20m from the center of the foundation (symmetrical axis). The soil at the base of the foundation experiences more significant heaving compared to the previous excavation phase.

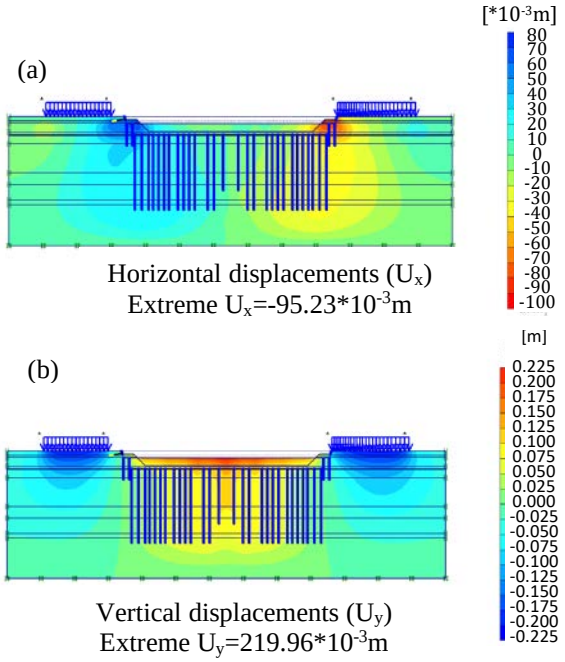

Fig. 6 Contour lines of displacement in the horizontal direction (a) and vertical direction (b) during excavation to the elevation of -4.0m

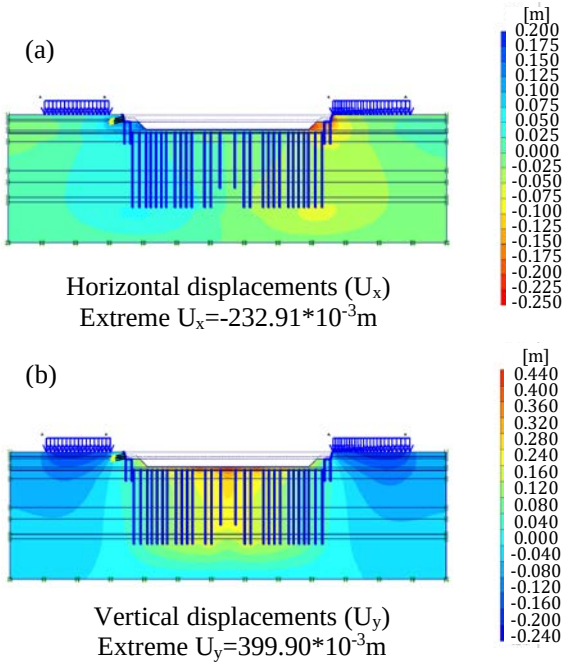

Fig. 7 Contour lines of displacement in the horizontal direction (a) and vertical direction (b) during excavation to the elevation of -8.0m

4.1.3. The excavation phase extends to a depth of -9.745m

Figure 8 illustrates that the element mesh becomes deformed when the excavation reaches a depth of -9.735 meters at the bottom of the pit.

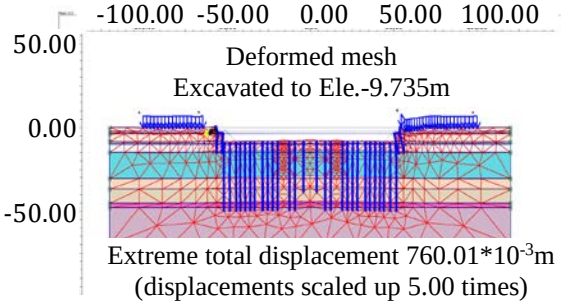

Fig. 8 Deformed mesh during excavation to the bottom of the foundation pit

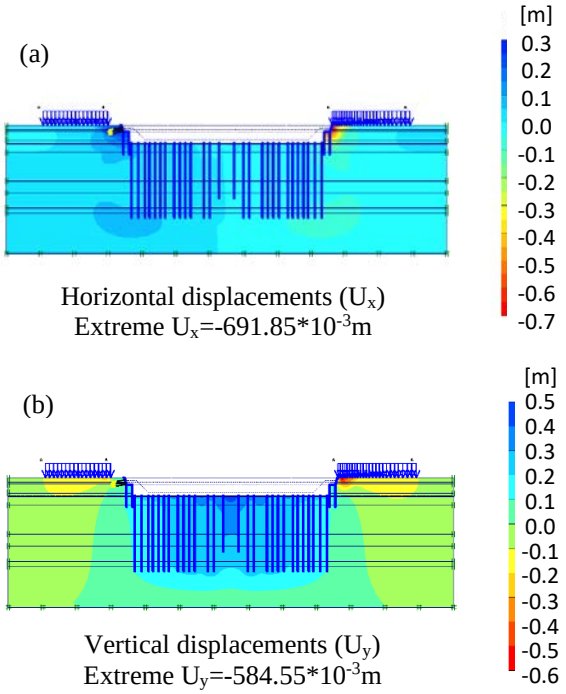

Fig. 9 Contours of (a) horizontal displacement and (b) vertical displacement during excavating to the bottom of the foundation pit (elevation of -9.735m)

Figure 9 displays the contours of horizontal and vertical displacements. Figure 9a represents the horizontal displacement of points on the pit's slope at the West and East sides. Within a range of approximately 12 meters from the edge of the excavation pit, the horizontal displacement at the West side is significantly greater than the horizontal displacement at the East side. Outside of this range, the differences in horizontal displacement between the two sides of the pit are negligible. It can be observed that the area influenced by the excavation in terms of horizontal displacement extends up to approximately 60 meters from the edge of the pit. The maximum vertical displacement reaches approximately 58.5cm near the top of the excavation pit (Fig. 9b). The ground at the bottom of the pit also experiences significant heaving, especially at the location close to the center of the excavation pit, with a vertical displacement of about 48cm.

These findings demonstrate the substantial deformation and displacement caused by the excavation process, which is critical to assessing its impact on both the ground and the nearby structures.

Figure 10 compares the horizontal displacements calculated using the finite element method at the ground surface at the West and East sides of the excavation pit. In general, the values on the pit's slope at the West side are higher than those at the East side within the vicinity of the pit.

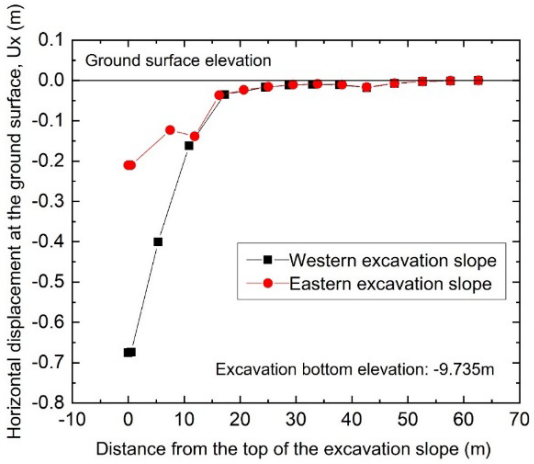

Fig. 10 Horizontal displacements at the ground surface of the excavation slopes on the East and West sides

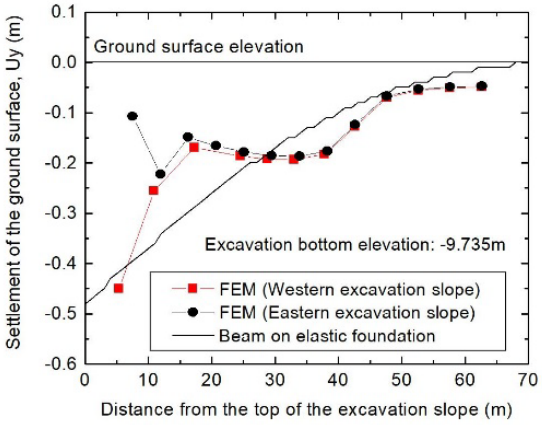

Fig. 11 Calculated settlement at the ground surface of the excavation slopes on the East and West sides

Figure 11 compares settlements calculated using the finite element method at the ground surface of the Western and Eastern sides of the excavation pit. Overall, the settlement value at the ground surface at Western excavation side is greater than that at the Eastern excavation side within the pit's vicinity.

It can be observed that at the excavation stage down to a depth of -9.735 meters, the settlement of the ground surface at the West side of the pit is

relatively significant. This could pose a danger to the stability of the structure and the nearby structures around the pit. Some settlement and cracking incidents have occurred in the surrounding residential buildings during the construction of this foundation pit. The reason could be that the West side of the pit's slope was not adequately reinforced, and the retaining wall at a depth of -9.735 meters might not have been constructed in a timely manner.

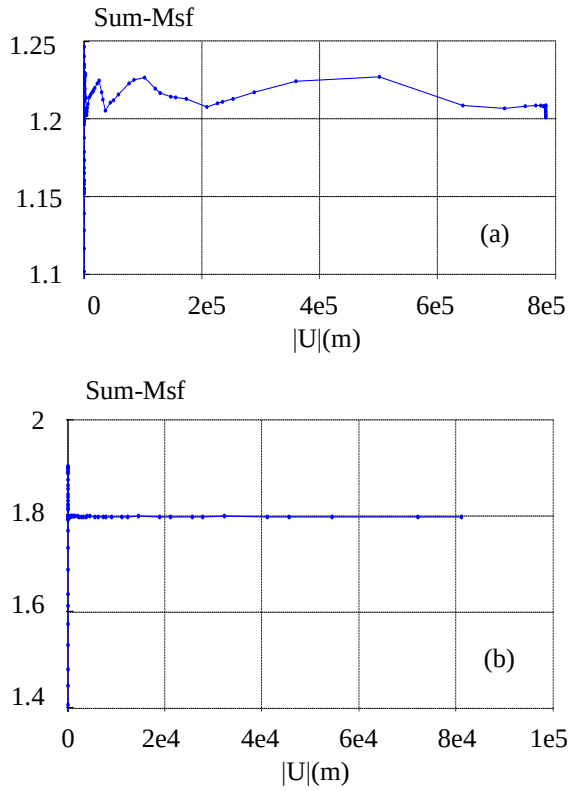

Fig. 12 The slope factors of stability against sliding of (a) the East-West cross-section and (b) the South-North cross-section during the excavation to the elevation of -9.735m

The excavation slope stability analysis was performed by finite element method with using the soil's shear strength reduction technique [15, 16]. The calculation result in Fig.12a indicates a stability safety factor of 1.21 at the designed excavation depth of -9.735m, which is relatively low.

It is evident that during the excavation phase down to the depth of -9.735m, significant ground displacement occurs at the western edge of the excavation. This poses a danger to the stability of the structure and the adjacent structures around the excavation because the western edge of the excavation is not reinforced by anchors, and the foundation raft at the depth of -9.735m has not been timely constructed.

4.2. FEM simulation of North-South cross section

4.2.1. Excavation down to the depth of -4.0m

Figure 13a shows the contour lines of horizontal displacement during excavation to the depth of -4.0m. The greatest horizontal displacement is approximately 6.2cm at the northern edge of the excavation (Thuy Khue Street side). Near this area, within about 10m from the excavation, the horizontal displacement approximates the highest value mentioned earlier. Figure 13b illustrates the contour lines of vertical displacement of the excavation. The maximum vertical displacement is around 17.8cm, occurring at the base of the foundation pit at the depth of -4.0m. At the foundation pit area, the ground is significantly heaved upwards.

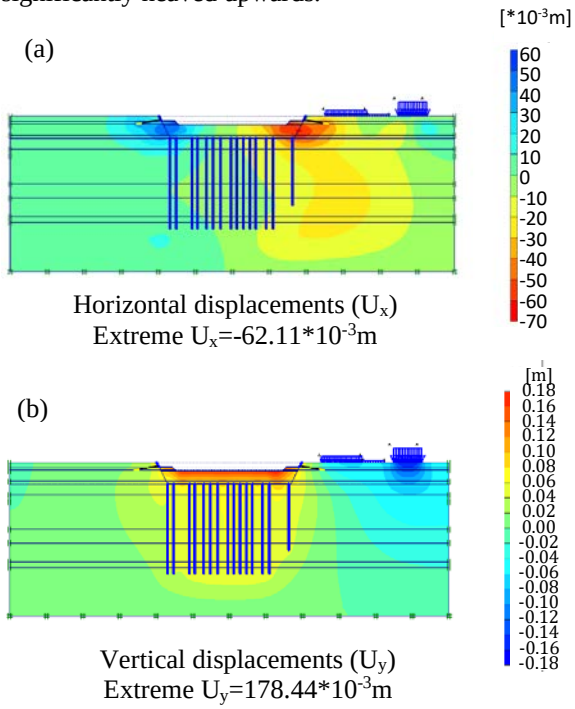

Fig. 13 Contour lines of (a) horizontal displacement and (b) vertical displacement during excavation to the elevation of -4.0m

4.2.2. Excavation down to the depth of -9.735m

Figure 14a exhibits the contour lines of horizontal displacement during excavation to the elevation of -9.735m. The highest horizontal displacement reaches approximately 14.6cm at the northern edge of the excavation. Within about 12m from the excavation, the horizontal displacement exceeds 10cm.

Generally, the horizontal displacement values at both the northern and southern edges are small. Figure 14b shows the contour lines of vertical displacement of the excavation. It is noticeable that the maximum vertical displacement, approximately 38.9cm, occurs at the base of the foundation pit, particularly in the area near the northern edge. At the foundation pit, the ground is significantly heaved upwards. Overall, the values of vertical displacement are not notably large.

The stability assessment against sliding was conducted using the technique of reducing the soil's shear strength. Figure 12b demonstrates a stability safety factor of about 1.8 at the designed excavation depth of -9.735m. This indicates a relatively high safety margin for the stability against sliding at the excavation's northern edge.

4.3. Beam on elastic foundation simulation

The modified Winkler model [5] as described above was applied to the project case of construction of excavation to the bottom foundation pit at elevation of -9.735m. It is assumed that the soil foundation property taken the property of soil layer 3. The simulation employed parameters are selected as follows: E=2717 kPa, v=0.35, L=0, H_k=9.735m, H_1=0.011H_k, k_r=0.8. a=0.7552, q=36 kPa, EJ=6.10^8 kN.m^2/m.

Figure 11 indicates that there is generally a good correlation in the settlement results when using the finite element method and elastic foundation method of beam on elastic foundation. This suggests that the calculated settlements align well with each other using these two different analysis approaches.

Hong Nam [17] compares the calculated settlement results of the ground surface using the elastic beam and finite element methods for scenarios with H_k=10m and 7m. In each comparison case, the parameters L and q are kept constant. He found that, within the vicinity of the excavation, both the elastic beam and finite element methods yield relatively suitable settlement results for a deep foundation pit (H_k=10m). However, farther from the excavation, in general, the settlement calculated using the elastic beam method is greater than that from the finite element one. For H_k=7m, generally, the settlement calculated by the elastic beam method is smaller than the corresponding values obtained using the finite element method.

Overall, within the vicinity of the excavation, settlement results obtained by both methods can be appropriate if the proper coefficients are selected. It is important to note that the finite element method holds an advantage over the elastic beam method because, in addition to settlement, it also provides results for horizontal soil displacement. In practical deep excavation construction, horizontal displacement is also of significant concern. Additionally, the elastic beam method does not consider the zone of influence on the ground surface, unlike the simulation by the finite element method [12]. To validate the settlement calculation results using different methods, field deformation measurements are required.

Significant influencing parameters on the settlement of the ground in the vicinity of deep excavation pits include the depth of the excavation pit, the distance from the edge of the pit to the nearby construction, and the applied load on the ground. In general, the settlement of the ground in the vicinity of construction increases as the depth of the excavation pit increases, the distance from the edge of the pit to the nearby construction decreases, and the applied load on the ground increases.

The limitation of the Mohr-Coulomb model is that it cannot distinguish between primary loading and unloading, and it overestimates the displacement during unloading. Note that the calculated settlements could be reduced if the unloading stiffness values of soils during the excavation stages were taken into account, along with the back calculation of soil stiffness [18-20]. Additionally, the stress anisotropies in soil stiffness were not considered.

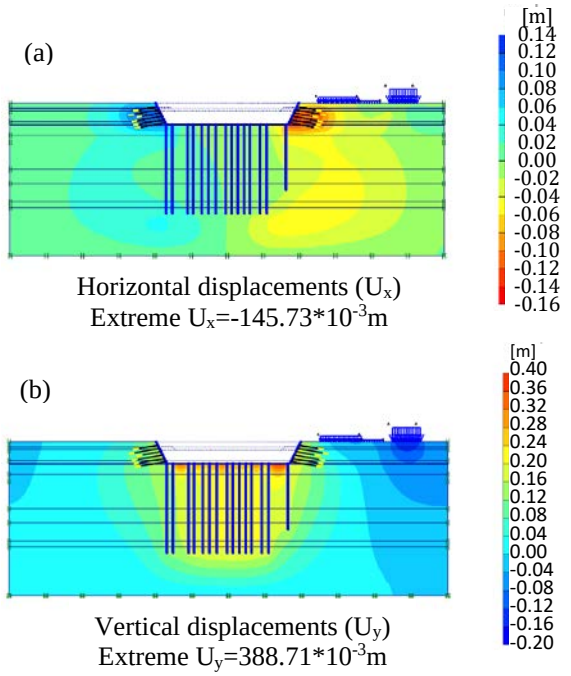

Fig. 14 Contour lines of (a) horizontal displacement and (b) vertical displacement during excavation to the elevation of -9.735m.

5. CONCLUSIONS

The incident of settlement and cracking of resident houses around a deep foundation pit of a high rise building by the open excavation method has been studied by the combination methods of site investigation, numerical and analytical simulations of stage construction for a real excavation problem. For the finite element simulation problem, two sections in the North-South and East-West directions were analyzed with plane strain problem, according to different excavation stages.

The simulation results showed that the measures to protect the western slope of the foundation pit by using only bored piles without reinforcing the slope of resident houses adjacent to the excavation pit led to the large ground deformation, endangering the

stability of the pit and the structure of the adjacent houses.

The computed deformations for the above project suggest that there is reasonable agreement between the ground settlement calculations in the vicinity of deep excavation pits using the methods of beam on elastic foundation and finite element.

Understanding the impact of deep excavations on the adjacent ground deformation and structures is crucial for ensuring the safety and stability of structures in urban environments.

6. REFERENCES

[1] Nguyen B. K., Construction of urban underground works using the open excavation method, Hanoi: Construction publishing House, 2008, pp. 5-8 (in Vietnamese).

[2] Di, H., Jin, Y., Zhou, S. et al., Experimental study on the adjustments of servo steel struts in deep excavations. Acta Geotech. Vol. 18, 2023, pp. 6615–6629, https://doi.org/10.1007/s11440-023-01959-5.

[3] Nangulama H.K., Jian Z., Xiao Z. et al., Stage-by-stage control effect field analysis of steel material servo enhanced support system on lateral displacement and bending moment during deep basement excavation, Case Studies in Construction Materials, Vol. 16, 2022, e01068, https://doi.org/10.1016/j.cscm.2022.e01068.

[4] Peck R. B., Advantages and Limitations of the Observational Method in Applied Soil Mechanics, Geotechnique, Vol. 19, Issue 2, 1969a, pp. 171-187. https://doi.org/10.1680/geot.1969.19.2.171

[5] Il'ichev V. A., Nikiforova N. S., and Koreneva E. B., Method for calculating bed deformation of buildings near deep excavations. Soil Mechanics and Foundation Engineering, Vol. 43, No.6, 2006, pp.189-196.

[6] Mana A. I. and Clough G. W., Prediction of Movements for Braced Cuts in Clay. J. of the Geotechnical Engineering Division, Vol. 107, Issue 6, 1996. https://doi.org/10.1061/AJGEB6.0001150.

[7] O'Rourke T. D., The ground movements related to braced excavations and their influence on adjacent buildings. US Department of Transport, DOT-TST76, T-23, 1976.

[8] Peck R. B., Deep Excavation and Tunneling in Soft Ground. State-of-the-Art Report. Proc. 7th Int. Conf. on Soil Mechanics and Foundation Engineering, Mexico, 1969b, pp. 225-290.

[9] Bauer G. E., Movements associated with the Construction of Deep Excavation. Proc. 3rd Int. Conf. Ground Mov. and Structures, Cardiff, 1984, pp. 694–706.

[10] Bowles J. E. Foundation Analysis and Design, 4th Edition, McGraw Hill, 1988, pp.658-661.

[11] Caspe M. S., Surface settlement adjacent to braced open cuts. Journal of the Soil Mechanics and Foundations Division, Vol. 92, No.4, 1966, pp. 51–59.

[12] Potts D. M. and Zdravkovic L., Finite element analysis in geotechnical engineering, Application, Thomas Telford, London, 2001, pp.74-124.

[13] GTC, Report on Geotechnical Investigation, Project: Hanoi Tung Shing club Project, Geotechnical research center, University of Mining and Geology, 2002, pp. 1-13.

[14] ADCOM, Documents determining ground displacement around the project during excavation construction. Project: Golden Westlake residence, Location: 151 Thuy Khue - Tay Ho – Hanoi, July 2007, pp.1-18 (in Vietnamese).

[15] Brinkgreve R. B. J., Broere W., and Waterman D., PLAXIS 2D- version 8, User's manual, Plaxis BV, The Netherlands, 2006.

[16] Matsui T. and San K. C., Finite element stability analysis by shear strength reduction technique. Soils and Foundations, Volume 32, No.1, 1992, pp. 59-70. https://doi.org/10.3208/sandf1972.32.59.

[17] Hong Nam N., Impact of deep excavation on the surface settlement of neighboring structures. Vietnam Geotechnical Journal, No. 4, 2009, pp. 38-47 (in Vietnamese).

[18] Hong Nam, N. and Dung, N.V., Effect of Deep Excavation on Deformation of Diaphragm Wall and Adjacent Structures. In: Duc Long, P., Dung, N. (eds) Geotechnics for Sustainable Infrastructure Development. Lecture Notes in Civil Engineering, vol. 62. (2020). Springer, Singapore. https://doi.org/10.1007/978-981-15-2184-3_42.

[19] Konstantakos D. C., Whittle A. J., Regalado C. et al., Control of ground movements for a multi-level-anchored, diaphragm wall during excavation. Proc. 5th Int. Conf. on Case Histories in Geotechnical Engineering, 37. New York, Univ. of Missouri—Rolla, 2004, https://scholarsmine.mst.edu/icchge/5icchge/session05/37/ .

[20] Rodriguez J.A., Deep excavation in soft soils and complex ground water conditions in Bogotá, Plaxis bulletin, Broere W. et al. (eds.), Issue 17, March, 2005, pp. 13-15.